IFASD 2015
International Forum on Aeroelasticity and Structural Dynamics
June 28 — July 02, 2015 ▲ Saint Petersburg, Russia

PREDICTION OF AEROELASTIC LIMIT-CYCLE OSCILLATIONS BASED ON HARMONIC FORCED MOTION OSCILLATIONS

A.C.L.M. van Rooij[1], J. Nitzsche[1] and R.P. Dwight[2]

[1]German Aerospace Center (DLR), Institute of Aeroelasticity
Bunsenstrasse 10, 37073 Göttingen, Germany
Anouk.vanRooij@dlr.de, Jens.Nitzsche@dlr.de

[2]Delft University of Technology, Faculty of Aerospace Engineering
Kluyverweg 1, 2629 HS Delft, The Netherlands
R.P.Dwight@tudelft.nl

Keywords: limit-cycle oscillations, aerodynamic non-linearities, fluid-structure interaction, p-k method

Abstract: Aeroelastic limit-cycle oscillations due to aerodynamic non-linearities are usually investigated using coupled fluid-structure interaction simulations in the time domain. These simulations can become computationally expensive, especially if the global bifurcation behaviour is of interest. To reduce the computational effort of parameter studies, an extension of the well-known p-k method is developed. In this frequency domain method, the aerodynamic forces and moments are now not only dependent on the frequency, but also on the oscillation amplitudes and the phase angle between the degrees of freedom. The first harmonic components of the aerodynamic forces are interpolated in the parameter space applying response surface modelling. The limit-cycle oscillation amplitude and mode shape are then found iteratively. The amplitude-dependent p-k method is verified and validated using an analytical testcase; the two-degree-of-freedom van der Pol oscillator. Excellent agreement with the time domain solution and the analytical solution is obtained. The amplitude-dependent p-k method is then applied to a two-degree-of-freedom airfoil system where the aerodynamic forces are computed from Euler simulations. Fluid-structure interaction simulations are performed for validation of the method. Both methods show good agreement in the bifurcation behaviour of the limit-cycle oscillation amplitude and mode shape.

1 INTRODUCTION

Limit-cycle oscillations (LCOs) are non-linear instabilities of an aeroelastic system. In contrast to classical flutter, the amplitude of an LCO does not grow unbounded, but remains constant due to the presence of a non-linearity. Limit-cycle oscillations are caused by either structural or aerodynamic non-linearities or a combination of both. Although their effect might not be immediately detrimental, as in the case of classical flutter, they can lead to fatigue of the aircraft's wings on the long term. In other words, if flutter is tolerated, because an LCO of small amplitude occurs at freestream velocities larger than the critical flutter speed, the flutter problem turns into a fatigue problem. Furthermore, the aeroelastic system might become unstable already at velocities lower than the critical flutter speed, i.e. limit-cycle oscillations might appear below the (linear) flutter boundary. Linear theory, however, which is used to predict classical flutter, fails to predict these instabilities.

Several researchers [1–4] have studied the limit-cycle oscillations that occur on the F-16 aircraft if external stores are applied. The driving mechanism of these LCOs has not been established yet, due the complicated non-linear behaviour. Aerodynamic sources of non-linearity are thought to be related to shock wave dynamics, flow separation and/or boundary layer transition. However, analysing the aerodynamic sources in detail is difficult by the use of numerical simulations, because of the high computational costs involved in coupled fluid-structure interaction (FSI) simulations in the time domain. Moreover, time domain simulations are not suited for detailed investigations into the bifurcation behaviour of LCOs. Unstable LCOs, for example, cannot be found using time domain simulations.

To ease the investigations into the behaviour of LCOs several alternative methods are used, such as the harmonic balance method [5]. Recently neural networks have also been applied to analyse limit-cycle oscillations with limited success ([6–8]). Another approach is to adapt the p-k-method, well-known in the context of a classical flutter analysis. Ueda et al. [9] first applied an adapted version of the p-k method in combination with the transonic small disturbance equations for predicting LCOs. They developed an extended non-linear indicial approach for modelling the aerodynamic forces. Thereby it was assumed that the frequency of the oscillation is low. The non-linear functions describing the aerodynamic forces were superposed. Good agreement with time domain simulations was obtained for small amplitude LCOs ($< 0.5°$). He et al. [10] recently applied a similar extended version of the p-k method, where superposition of the aerodynamic forces is also applied. Computational Fluid Dynamics (CFD) was used to compute the aerodynamic forces and hence the low frequency assumption is dropped compared to Ueda et al. [9]. The method of He et al. [10] was successful if the non-linearity is weak. However, for stronger non-linearities, deviations compared to other methods (time domain, harmonic balance) are present.

In contrast to the methods of Ueda et al. [9] and He et al. [10], in this work an adapted p-k method is presented in which the amplitude dependency of the aerodynamic forces is taken into account directly by the use of harmonic forced motion oscillations. Hence, no superposition of the aerodynamic forces is applied. The LCO is assumed to oscillate with its first fundamental frequency (as in [9, 10]), i.e. the higher order harmonic components of the LCO and the aerodynamic forces are neglected. The results of the adapted p-k method are compared to time domain simulations results. Before applying the amplitude-dependent p-k method to a CFD testcase, it is verified for an analytical testcase; a two-degree-of-freedom (DOF) van der Pol-oscillator [11] system. Afterwards the method is applied to a two DOF pitch/plunge airfoil system.

Section 2 describes the amplitude-dependent p-k method, the CFD code and the time domain method used as a reference. Then, the results of amplitude-dependent p-k method are shown and discussed in section 3 for the two DOF van der Pol-oscillator and the two DOF airfoil system. Finally, conclusions are drawn.

2 METHODS

In this work two methods have been applied, a time domain and a frequency domain method. The frequency domain method used here is an extension of the well-known p-k method used for flutter computations. In the time domain fluid-structure coupling has

been applied for validation of the frequency domain method. This section first describes the aeroelastic systems considered in this work, then both methods will be presented.

2.1 van der Pol-oscillator

The van der Pol-oscillator is a classical example of a system with a non-linear damping force and serves here as a model for non-linear aerodynamic forces. The standard van der Pol oscillator with one degree of freedom has been extended to two degrees of freedom. Furthermore, the non-linear damping force has been extended with a fourth order term. The equations of motion are given by:

$$\mathbf{M}\ddot{\vec{x}} + \mathbf{K}\vec{x} = \epsilon \begin{bmatrix} \mu - a_1 x_1^2 - b_1 x_1^4 & \mu - a_2 x_1^2 \\ \mu - a_3 x_2^2 & \mu - a_4 x_2^2 - b_2 x_2^4 \end{bmatrix} \begin{bmatrix} \dot{x}_1 \\ \dot{x}_2 \end{bmatrix} \tag{1}$$

where $\vec{x} = [x_1, x_2]^T$ is now a vector with the displacements of the two degrees of freedom and a_1, a_2, a_3, a_4, b_1 and b_2 are constants. $\mathbf{M}$ and $\mathbf{K}$ are the mass and stiffness matrices, respectively and ϵ is a damping coefficient used to scale the damping.

2.2 Two degree-of-freedom airfoil system

The aeroelastic system considered in this work is an airfoil with two degrees of freedom; pitch and plunge. A sketch of this aeroelastic system is shown in Figure 1. The equations of motion of the system are given by:

$$\begin{bmatrix} m & S_\alpha \\ S_\alpha & I_\alpha \end{bmatrix} \begin{bmatrix} \ddot{h} \\ \ddot{\alpha} \end{bmatrix} + \begin{bmatrix} d_h & 0 \\ 0 & d_\alpha \end{bmatrix} \begin{bmatrix} \dot{h} \\ \dot{\alpha} \end{bmatrix} + \begin{bmatrix} k_h & 0 \\ 0 & k_\alpha \end{bmatrix} \begin{bmatrix} h \\ \alpha \end{bmatrix} = \begin{bmatrix} -L \\ M \end{bmatrix} \tag{2}$$

where m is the mass, I_α the mass moment of inertia, S_α the static moment, k_h the plunge stiffness, k_α the torsional stiffness, d_h is the plunge damping and d_α is the torsional damping. The aerodynamic force vector $\vec{f}$ consists of the aerodynamic lift L and the moment M. The vertical displacement is denoted by h and the angle of attack by α. The airfoil used in this work is the NLR7301 airfoil. This airfoil has been used for various wind tunnel tests [12–16] and numerical investigations [17–27].

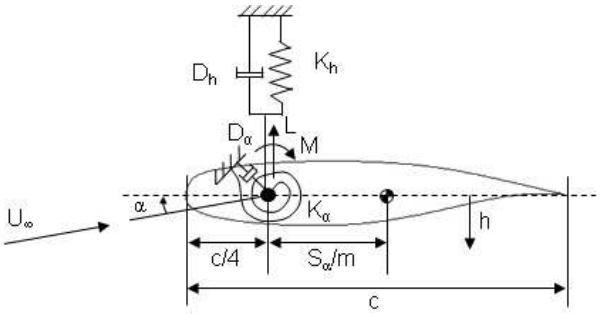

Figure 1: Sketch of the airfoil model with two degrees of freedom

2.3 CFD code and set-up

The aerodynamic lift and moment are determined using the DLR TAU-code [28] in its Euler mode. This Computational-Fluid Dynamics (CFD) code is a finite-volume, cell-vertex-based, unstructured solver for both the Reynolds-Averaged Navier-Stokes and the Euler equations. For spatial discretisation a 2nd order central scheme [29] is used. Temporal discretisation is realised by dual time stepping [30] with the 2nd order accurate Backward Differencing Formula (BDF2) integration scheme for the physical time.

The airfoil used in this study is the supercritical NLR7301 airfoil with a blunt trailing edge [31]. Its design Mach number is 0.72 and its design lift coefficient is 0.60. The unstructured O-type mesh used for all CFD simulations has 1135 points. The farfield boundary has been placed 100 chord lengths away from the airfoil, in order to avoid that reflections falsify the low frequency responses. The time step size used for all unsteady simulations is $1 \cdot 10^{-4}$ s. This time step size was found to give time step size independent results in a previous study [32].

2.4 Time domain

2.4.1 Fluid-structure coupling

Limit-cycle oscillations are computed in the time domain using fluid-structure coupling. The time integration is performed using a BDF2 integration scheme. The coupling is partitioned, however, it is strong. The forces and displacements are exchanged between the CFD solver and the equation-of-motion solver at each pseudo time step. In order words, at a certain time step, the forces of the previous physical or pseudo time step are used to compute the new structural displacements. These are then fed back to the CFD code to compute the new aerodynamic forces at the current pseudo time step, which then lead to new displacements. These are again fed back to the CFD code. This process is repeated for each pseudo time step until an equilibrium is established at a certain time step. Then the solver advances to the next time step. In order to obtain the desired mean angle of attack, the airfoil is "trimmed" at a certain angle of attack by subtracting the static aerodynamic forces and (mean) angle of attack.

2.4.2 Harmonic forced motion oscillation simulations

Harmonic forced motion oscillation simulations are performed to obtain the frequency response function (FRF), or the describing function (DF) in the non-linear case, of the aerodynamic forces. The airfoil performs a harmonic motion, this can be either a pitching motion, a plunging motion or a combination of both. Equations (3) and (4) represent the time signal of the angle of attack α and the vertical position h.

$$h(t) = \Delta h \cdot \sin(\omega t + \Delta\phi) \tag{3}$$

$$\alpha(t) = \Delta\alpha \cdot \sin(\omega t) \tag{4}$$

In equations (3) and (4), $\Delta\alpha$ is the pitch amplitude and Δh is the plunge amplitude. The phase difference between both degrees of freedom is denoted by $\Delta\phi$. In contrast

to the linear case, in which the principle of superposition can be used to compute a combined pitch/plunge response, in the non-linear case both motions need to be simulated simultaneously to account for non-linear higher order coupling terms. Furthermore, the amplitudes of the both pitch and plunge as well as the phase difference between both motions need to be taken into account. Hence, the outcome of the harmonic forced motion oscillations described here, is not a describing function in the classical sense, since the lift and moment are not only dependent on the frequency and the amplitude, but also on the complex amplitude ratio between the degrees of freedom.

In the amplitude-dependent p-k method, only the first harmonics of the motion and the aerodynamic response are taken into account. Although there are significant higher harmonics in the aerodynamic response, the work they perform on the airfoil is negligible, since the higher harmonics in the motion of the structure are very small compared to the first harmonic component (see [33]). Furthermore, the higher harmonics in the aerodynamic response do not perform work on the first harmonic of the structural motion. Therefore, taking into account the first harmonics of the aerodynamic forces is sufficient if the LCO is (almost) first harmonic. If the LCO has significant higher order components it is expected that the amplitude-dependent p-k method will fail to predict the correct LCO amplitude. However, these LCOs were not observed from CFD simulations and experiments with aerodynamic non-linearities only [13, 15, 16, 32, 33].

2.5 Frequency domain

The conventional p-k method, developed by Hassig [34], as used for classical flutter computations cannot be used for predicting the occurrence of limit-cycle oscillations. At least not in its original form, since the aerodynamic forces are no longer a linear function of the displacements. In the extended p-k method a harmonic solution to the equations of motion (2) of the form:

$$\vec{x} = \vec{\hat{x}} e^{pt}, \tag{5}$$

is assumed similar to the conventional p-k method. Here $\vec{\hat{x}}$ indicates the complex-valued eigenvector and p is a complex-valued eigenvalue, defined by:

$$p = \delta + i\omega, \tag{6}$$

where δ is the damping and ω the angular frequency. The non-dimensional reduced frequency k is computed from the angular frequency via $k = \omega c/U_\infty$. For the aerodynamic response of the system only the first harmonic component is considered, since the other harmonics are not of interest (as explained in section 2.4), i.e.:

$$\vec{f} = \vec{\hat{f}} e^{i\omega t} = \vec{\hat{f}} e^{i\frac{kU_\infty}{c}t} \tag{7}$$

where $\vec{\hat{f}}$ is the complex amplitude vector of the aerodynamic force. Substituting the assumed solution (equations (5) till (7)) into the equations of motion (equation (2)) yields:

$$p^2\mathbf{M}\vec{\hat{x}} + p\mathbf{D}\vec{\hat{x}} + \mathbf{K}\vec{\hat{x}} = \vec{\hat{f}}\left(k,\, \vec{\hat{x}}\right). \tag{8}$$

Now in the conventional p-k method the right-hand side vector is written as a Generalised Airforce (GAF)-matrix times the eigenvector. In case of an LCO, this is no longer possible, since the amplitude-dependency of the aerodynamic forces needs to be taken into account. The aerodynamic force vector is now not only a non-linear function of the frequency, but also a non-linear function of the mode shape, that is, of the amplitudes of both degrees of freedom and the complex amplitude ratio. Therefore, $\vec{\hat{x}}$ is now called the mode shape vector and equation (8) needs to be solved iteratively using Newton's method for example.

In order to uniquely determine the mode shape vector $\vec{\hat{x}}$ one of the amplitudes (either pitch or plunge) is pre-set. The mode shape vector then becomes:

$$\vec{\hat{x}} = \begin{bmatrix} \frac{\Delta h}{\Delta \alpha} \cdot e^{(\Delta\phi \cdot i)} \\ 1 \end{bmatrix} \cdot \Delta\alpha. \tag{9}$$

Then equation (8) is solved for two unknowns: the complex eigenvalue p and the complex amplitude ratio $\frac{\Delta h}{\Delta \alpha} \cdot e^{(\Delta\phi \cdot i)}$. This is done for each pre-set amplitude ($\Delta\alpha$ or Δh, here $\Delta\alpha$ has been used). Since the force vector depends on the frequency and on the mode shape, the equations of motion need to be solved iteratively. Hence, similarly as for the conventional p-k method the following steps are performed:

1. Choose a certain reduced frequency k and mode shape vector $\vec{\hat{x}}$ (i.e. a complex amplitude ratio $\frac{\Delta h}{\Delta \alpha} \cdot e^{(\Delta\phi \cdot i)}$)
2. Compute the aerodynamic force vector at this frequency and mode shape (by interpolation)
3. Solve the system of equations (8) for p and $\vec{\hat{x}}$
4. Take new $k = \Im(p)$ and $\vec{\hat{x}} = [\frac{\Delta h}{\Delta \alpha} \cdot e^{(\Delta\phi \cdot i)},\, 1]^T \cdot \Delta\alpha$
5. Iterate until converged

This procedure is repeated for each pre-set amplitude $\Delta\alpha$. The amplitude $\Delta\alpha$ at which the damping is zero is the LCO amplitude. The other LCO properties (plunge amplitude Δh, amplitude ratio $(\Delta h/c)/\Delta\alpha$ and the phase difference $\Delta\phi$) are determined from the mode shape vector $\vec{\hat{x}}$ and the reduced frequency is determined from p. Figure 2 schematically presents the possible damping curves that result from a computation with the amplitude-dependent p-k method. The pre-set amplitude is depicted on the horizontal axis. Positive damping indicates a motion growing in amplitude, negative damping indicates a motion decaying in amplitude. The blue curve shows a positive damping at low amplitudes, then the damping becomes negative with increasing amplitude. The LCO that occurs at zero damping is stable, it is an attractor. The red curve shows two intersections with the horizontal axis. One from negative to positive damping and one from positive to negative damping with increasing amplitude, i.e. an unstable and a stable LCO occur. The unstable LCO is a repeller as indicated by the arrows.

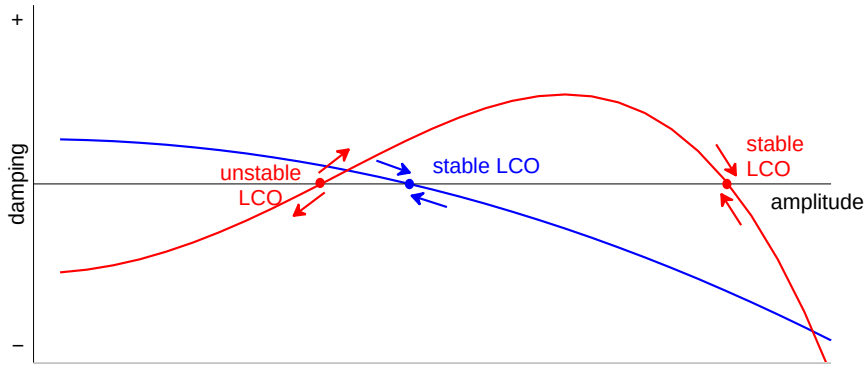

Figure 2: Sketch of damping versus amplitude

The amplitude-dependent p-k method as described here can be used to determine the LCO amplitude when the describing function is known as a function of the frequency, pitch amplitude, plunge amplitude and the phase difference between pitch and plunge. In order to determine the aerodynamic lift and moment at each combination of amplitudes, frequency and phase difference, a so-called response surface is built using harmonic forced motion CFD simulations. Interpolation on this response surface is then applied during the iterations of the amplitude-dependent p-k method.

The harmonic forced motion oscillation simulations are uniformly spaced in all four dimensions (reduced frequency, amplitude ratio, phase difference, pitch amplitude). For interpolation the Matlab-toolbox DACE [35] has been used. Using this toolbox simple Kriging has been applied. In Kriging, the model for an unpredicted site consists of the sum of a regression model and a random process. In simple Kriging the regression model is just a constant. The random process is assumed to have a zero mean. The covariance of the random process is modelled using a so-called correlation function. In this work two correlation functions were used: the linear and the spline correlation functions. More details on Kriging can be found in [36].

3 RESULTS AND DISCUSSION

This section shows the results obtained from the amplitude-dependent p-k method. The results are validated using FSI simulations. First, the results of the van der Pol-oscillator testcase are shown and discussed. Then the results of the two-degree-of-freedom airfoil system are shown and discussed.

3.1 van der Pol-oscillator

The equations of motion of the two-degree-of-freedom van der Pol system are given in equation (1). These equations can be solved either in the time domain or in the frequency domain. When the non-linear damping force vector is reduced to a non-linear damping force in the first (or second) DOF only, an analytical solution is available. Therefore, for validations purposes, the coefficients a_2, a_3, a_4, b_1 and b_2 have been set to zero. The other coefficients have been taken as follows: $\epsilon = 0.02$, $a_1 = 0.3$. The mass matrix has been set to the identity matrix and the stiffness matrix is defined as:

$$\mathbf{K} = \begin{bmatrix} 20 & -10 \\ -10 & 10 \end{bmatrix} \tag{10}$$

The analytical solution for the LCO amplitude can be computed using the principle of energy conservation. Since the non-linear damping force is only present in the first equation, the LCO amplitude of the other degree of freedom is computed using the absolute value of the complex amplitude ratio. Equations (11) and (12) present the analytical solution to equation (1).

$$\Delta x_1 = \left| \frac{\Delta x_1}{\Delta x_2} \cdot e^{i\Delta\phi} \right| \cdot 2\sqrt{\frac{\mu}{a_1}} \tag{11}$$

$$\Delta x_2 = 2\sqrt{\frac{\mu}{a_1}} \tag{12}$$

The amplitude-dependent p-k method has been used to study the bifurcation behaviour of the 2 DOF van der Pol oscillator by varying the parameter μ. Two unstable modes were observed from all methods, one at an angular frequency of 1.95 rad/s and one at an angular velocity of 5.14 rad/s. In Figure 3 the LCO amplitude is plotted as a function of μ. The symbols show the LCO amplitude as obtained from the amplitude-dependent p-k method, whereas the dashed lines show the analytical solution. Δx_1 and Δx_2 represent the amplitudes of the first and second degree of freedom, respectively. The red pentagrams and green hexagrams show the time domain results, for the first and second DOF, respectively. Matlab's ode45 solver has been used to obtained these time domain results.

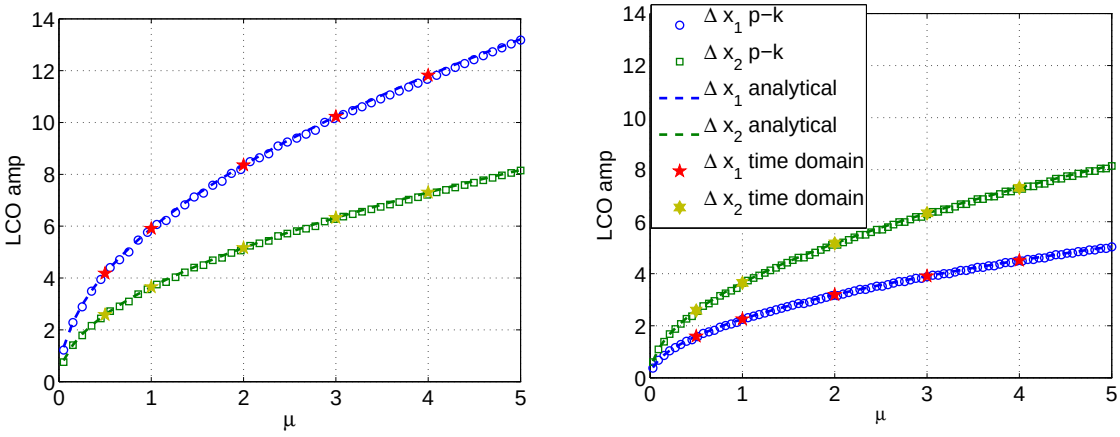

(a) Mode 1: $\omega = 1.95$ rad/s

(b) Mode 2: $\omega = 5.14$ rad/s

Figure 3: Bifurcation diagrams of the two degree-of-freedom van der Pol oscillator system ($\epsilon = 0.02$, $a_1 = 0.3$ and $a_2 = a_3 = a_4 = b_1 = b_2 = 0$)

The LCO amplitude increases with increasing bifurcation parameter μ, i.e. a supercritical bifurcation of the LCO amplitude occurs. Furthermore, excellent agreement is observed between the analytical, time domain and the frequency domain solutions. Hence, the amplitude-dependent p-k method can be used to estimate the LCO amplitude and the LCO mode shape.

The influence of a fourth order non-linear damping term in the van der Pol oscillator system has been investigated. The following values for the coefficients a_2 till b_2 have been used: $\epsilon = 0.002$, $a_1 = -6$, $a_2 = -2$, $a_3 = -1$, $a_4 = -4$, $b_1 = 0.25$ and $b_2 = 0.5$. Solving equation 1 a subcritical bifurcation is obtained, see Figure 4. Again both modes become unstable. Mode 1 has an angular frequency of 1.96 rad/s and mode 2 an angular frequency of 5.12 rad/s. The red pentagrams and green hexagrams in Figure 4(a) show the time domain results. The second mode was not found from time domain simulations. The black arrows in Figure 4(a) indicate path that is followed when μ is changed.

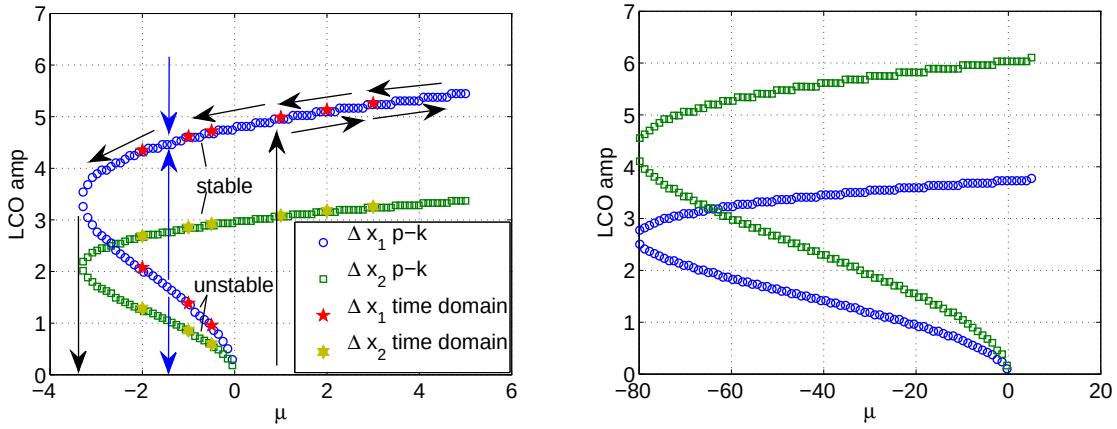

(a) Mode 1: $\omega = 1.96$ rad/s

(b) Mode 2: $\omega = 5.12$ rad/s

Figure 4: Bifurcation diagrams of the two degree-of-freedom van der Pol oscillator system ($\epsilon = 0.002$, $a_1 = -6$, $a_2 = -2$, $a_3 = -1$, $a_4 = -4$, $b_1 = 0.25$ and $b_2 = 0.5$)

From Figure 4 it is observed that for both modes a subcritical bifurcation occurs, i.e. for values of μ smaller than zero two LCOs exist, a stable and an unstable. For μ larger than zero, only one LCO exists, a stable LCO. The blue arrows indicate that the stable LCO is an attractor, whereas the unstable LCO is a repeller. This repellor can in principle not be found from time domain simulations. For validation purposes, it has been determined here by reversing the sign of the non-linear damping term in the time domain computations.

3.2 2 DOF airfoil system

The amplitude-dependent p-k method has been applied to a two-degree-of-freedom airfoil system. The aerodynamic forces were computed using CFD simulations solving the Euler equations. Harmonic forced motion simulations were performed sampling the parameter space spanned by reduced frequencies, amplitude ratios, phase differences between pitch and plunge and pitch amplitudes. The results are used to create a response surface, which is used for the determination of the aerodynamic forces in the amplitude-dependent p-k method. For validation, the LCO amplitude has been determined at several freestream velocities from FSI simulations in the time domain. The testcase considered in this work is at a Mach number of 0.74 and a mean angle of attack of $-1.5°$. The structural parameters used are given in Table 1.

Structural parameter	Value
Mass m	$26.268\,\mathrm{kg}$
Mass moment of inertia I_α	$0.079\,\mathrm{kg/m^2}$
Torsional spring stiffness k_α	$6.646 \cdot 10^3\,\mathrm{Nm/rad}$
Plunge spring stiffness k_h	$1.078 \cdot 10^6\,\mathrm{N/m}$
Static moment related to EA S_α	$0.331\,\mathrm{kgm}$
Torsional damping constant d_α	$0.0687\,\mathrm{kgm^2/s}$
Plunge damping constant d_h	$45.764\,\mathrm{kg/s}$

Table 1: Structural parameters for the 2 DOF NLR7301 airfoil system

The amplitude-dependent p-k method has been used to compute the LCO amplitude and mode shape. The samples used for the creation of the response surface are shown in Table 2. The simplest possible sampling method, uniform sampling has been chosen for the sampling. In addition to the non-linear samples shown in Table 2, samples at very small amplitude (0.001°) were computed from superposition of the linear frequency response functions that were used for determining the linear stability. Note from Table 2 that more samples are used for the pitch amplitude than for the other mode shape parameters. This choice is based on the results of forced motion simulations with dense sampling of a certain mode shape parameter, while keeping all other mode shape parameters fixed. The magnitude and phase of the lift and moment varied the most with the reduced frequency and pitch amplitude. Figure 5 shows the magnitude and phase angle of the lift versus the pitch amplitude for an amplitude ratio of 0.5, a reduced frequency of 0.3 and a phase difference of 5°. The symbols show the samples of the forced motion simulations in the time domain, the dashed blue line the linear interpolation and the dashed red line the spline interpolation as obtained from DACE. The phase angle of the lift shows very non-linear behaviour with varying pitch amplitude. Therefore it was decided to apply dense sampling for this mode shape parameter. The magnitude of the lift shows a nearly linear dependency on the pitch amplitude. Although, there is a non-linear variation of the aerodynamic forces with the reduced frequency, as in a classical flutter analysis, no dense sampling was applied for this parameter, since for this testcase the LCO reduced frequency is close to the sample point at 0.3.

Mode shape parameter	Values
Pitch amplitude $\Delta\alpha(^\circ)$	0.1, 0.5, 1, 1.5, 2, 3, 4, 5
Amplitude ratio $(\Delta h/c)\,/\Delta\alpha$	0.1, 0.5, 1
Reduced frequency k	0.2, 0.3, 0.5
Phase difference $\Delta\phi$ (°)	-10, -5, 5, 10

Table 2: Values of the mode shape parameters used for determination of the response surface of 2 DOF NLR7301 airfoil system

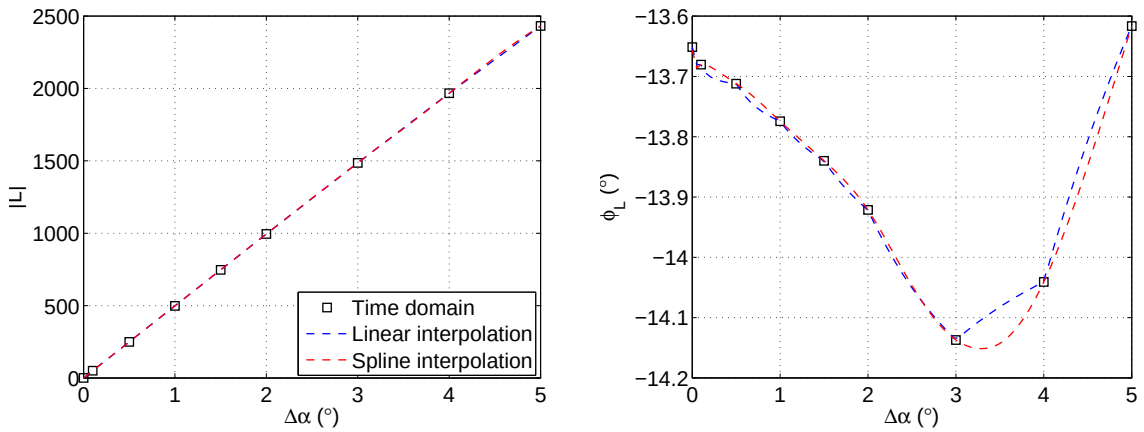

(a) Magnitude (b) Phase angle

Figure 5: Magnitude and phase angle of lift versus the pitch amplitude at $(\Delta h/c)/\Delta\alpha = 0.5$, $\Delta\phi = 5°$, $k = 0.3$

Using the samples as depicted in Table 2 (and the linear samples), the amplitude-dependent p-k method has been applied using two different interpolation techniques. Kriging has been applied for the interpolation with a linear correlation model and with a spline correlation model. The amplitude at which the damping becomes zero has been determined for several freestream velocities. The results are plotted in Figure 6 together with the results from fluid-structure interaction simulations. Since it takes a lot of computational effort to determine the LCO amplitude in the time domain, several FSI simulations at various initial amplitudes have been performed for each freestream velocity. From each of these simulations it has been determined whether the oscillation amplitudes of the system where growing or decaying. In that manner, the bounds between which the LCO amplitude lays have been determined. The blue circles and the red squares depict the lower and upper bounds between which the LCO occurs. The blue circles at zero amplitude show the results of FSI simulations for which the amplitude decays towards zero. The green solid and blue dashed lines in Figure 6 show the frequency domain solution using linear and spline interpolation, respectively. The linear flutter velocity obtained from the p-k method (using linear interpolation) is plotted in Figure 6 with a green diamond at a zero amplitude.

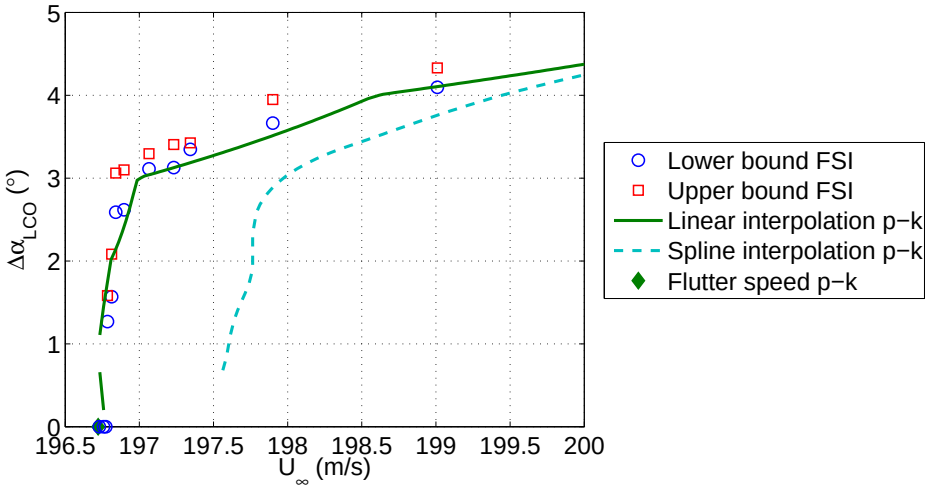

Figure 6: LCO amplitude versus freestream velocity

From the time domain simulations it is seen that the LCO amplitude increases with increasing freestream velocity, i.e. a supercritical bifurcation occurs. Below a freestream velocity of approximately 196.73 m/s all FSI simulations decay towards zero amplitude, i.e. no LCOs occur. The agreement of the results of the amplitude-dependent p-k method with the time domain results is very good when linear interpolation is applied. In case of spline interpolation, the bifurcation diagram is shifted to slightly higher velocities (about 1 m/s). This is explained by the interpolation of the response surface. It was observed that the spline interpolation of the response surface is not optimal in all dimensions, i.e. more samples are probably necessary for the spline interpolation to better predict the LCO amplitude. From the linear curve it is clearly visibly at which positions a sample has been placed (see for example the kinks at $\Delta\alpha = 3°$ and $4°$). Hence, the interpolation method needs to be improved (as was also seen from Figure 5(b)). When linear interpolation is applied, both stable and unstable LCOs occur at small amplitudes. This is attributed to the number of samples used for the generation of the response surface and the interpolation method applied on the response surface. However, except for these small amplitudes, the bifurcation type obtained with amplitude-dependent p-k method is also supercritical. Figure 7 shows the other LCO mode shape parameters (amplitude ratio, reduced frequency and phase difference between pitch and plunge) as obtained from the amplitude-dependent p-k method versus the freestream velocity. For comparison the time domain results are also shown.

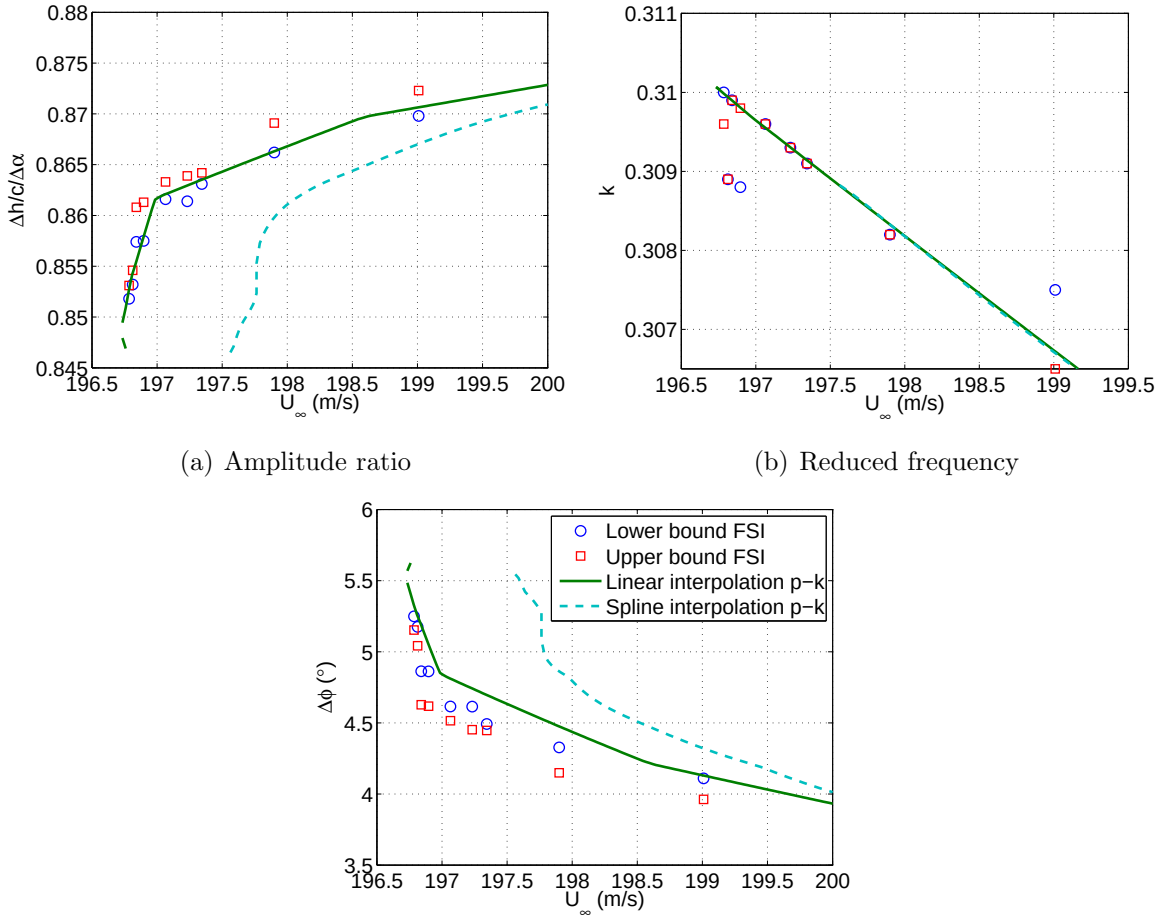

(a) Amplitude ratio

(b) Reduced frequency

(c) Phase difference

Figure 7: LCO mode shape versus freestream velocity

Figure 7 shows a supercritical bifurcation of the amplitude ratio with the freestream velocity. The reduced frequency is monotonically decreasing with freestream velocity. Although it should be noted that the variation of reduced frequency with freestream velocity is minimal. The phase difference decreases with increasing freestream velocity, meaning that the pitching and plunging motions tend to get more in phase. The small positive phase difference indicates that pitch is leading plunge. The bifurcation behaviour of the LCO mode shape is globally correctly predicted by the amplitude-dependent p-k method as can be seen from Figure 7. The agreement between the FSI results and those obtained from the p-k method with linear interpolation are very good. The results obtained with spline interpolation show the same trends as the time domain results. However, the curves are slightly shifted. For larger amplitudes the frequency domain results come closer to the time domain results.

Since interpolation of the first harmonic of the aerodynamic forces is applied, it is interesting to look at these forces during the LCO. Figure 8 shows the magnitude and phase angle of the lift and moment during the LCO as a function of the freestream velocity. Both time and frequency domain results are presented. Similar trends are observed. The magnitude of the lift and moment are seen to increase with freestream velocity. The phase of the lift first decreases sharply and then increases. This is also predicted by the amplitude-dependent p-k method. The phase of the moment decreases monotonically.

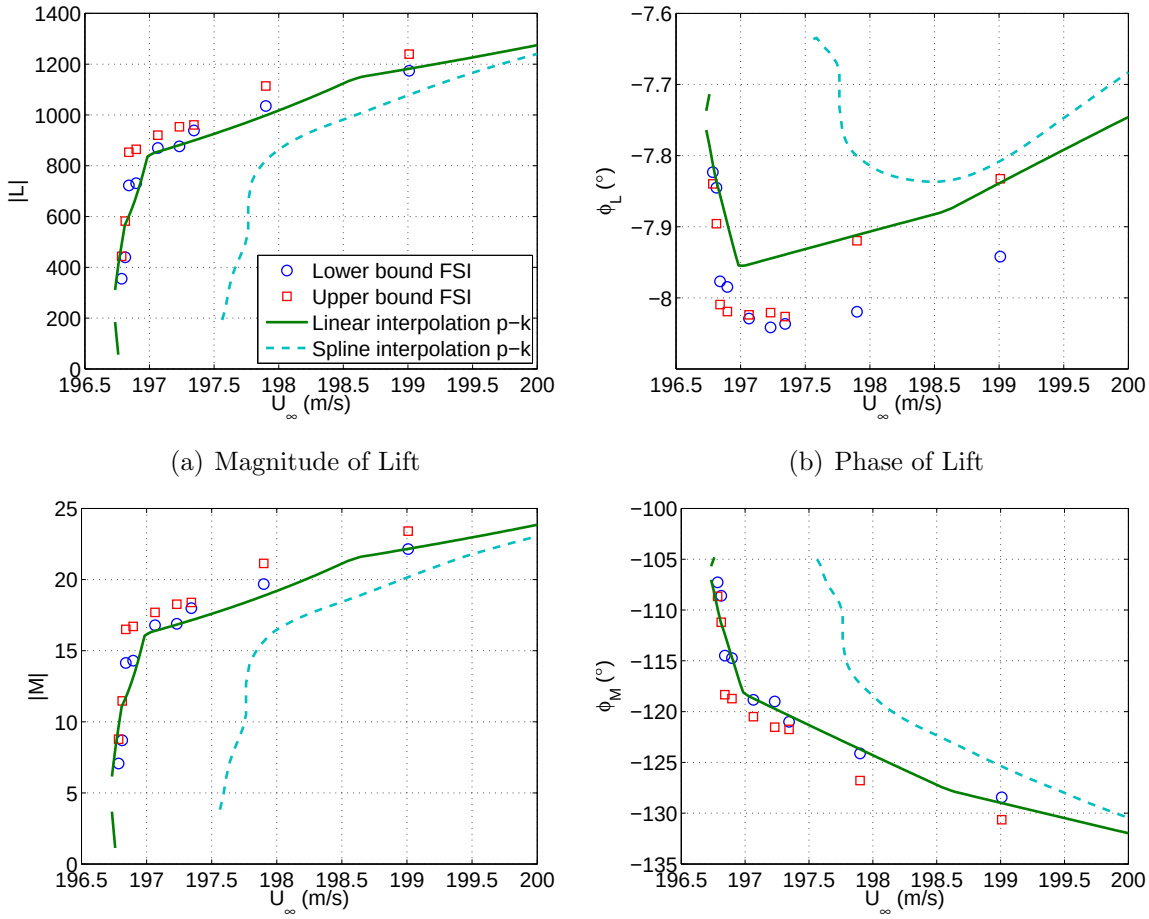

(a) Magnitude of Lift

(b) Phase of Lift

(c) Magnitude of Moment

(d) Phase of Moment

Figure 8: Magnitude and phase angle of aerodynamic forces during LCOs versus freestream velocity

Overall the agreement between the results of the amplitude-dependent p-k method and the coupled time simulations is good for both testcases considered in this work. Hence, the amplitude-dependent p-k method is suitable alternative for studying limit-cycle oscillations.

4 CONCLUSION

In this work an alternative method for the prediction of limit-cycle oscillations has been presented. This amplitude-dependent p-k method takes into account the first harmonic of the aerodynamic forces as a function of the frequency, amplitude, amplitude ratio and phase difference between the degrees of freedom. The method developed has been verified and validated for two testcases: a two-degree-of-freedom van der Pol-oscillator and a two-degree-of-freedom airfoil system.

The two DOF van der Pol oscillator testcase showed an excellent agreement between the time domain, frequency domain and the analytical solution. Adding a fourth order damping term, resulted in a subcritical bifurcation behaviour of the LCO amplitude. This indicates that to obtain a subcritical bifurcation in a two DOF airfoil system, the aerodynamic damping should locally be approximately a polynomial of order four. Furthermore, this demonstrates that unstable LCOs can be found using the amplitude-dependent p-k

method.

For the two degree-of-freedom airfoil system a response surface for the aerodynamic forces has been built using harmonic forced motion simulations. This response surface has been used to determine the aerodynamic forces during the iterations of the p-k method. From both the time domain and frequency domain simulations a supercritical bifurcation is observed. The agreement between the LCO amplitude and mode shape obtained from both methods is good. Hence, the amplitude-dependent p-k method can be used to estimate limit-cycle oscillations. Furthermore, taking into account only the first harmonic component of the aerodynamic forces is sufficient for the LCOs observed in this work. Therefore, once a response surface has been built for a certain Mach number and mean angle of attack, structural parameter studies can be easily performed using the amplitude-dependent p-k method.

5 REFERENCES

[1] Denegri, C. (2000). Limit cycle oscillation flight test results of a fighter with external stores. *Journal of Aircraft*, 37(5), 761–769.

[2] Bunton, R. and Denegri, C. (2000). Limit cycle oscillation characteristics of fighter aircraft. *Journal of Aircraft*, 37(5), 916–918.

[3] Dreyer, C. and Shoch, D. (1986). F-16 flutter testing at eglin air force base. AIAA-86-9819. Las Vegas, NV, USA. 3rd Flight Testing Conference.

[4] Chen, P., Sarhaddi, D., and Liu, D. (1998). Limit-cycle-oscillation studies of a fighter with external stores.

[5] Hall, K., Thomas, J., and Clark, W. (2002). Computation of unsteady nonlinear flows in cascades using a harmonic balance technique. *AIAA Journal*, 40.

[6] Balajewicz, M. and Dowell, E. (2012). Reduced-order modeling of flutter and limit-cycle oscillations using the sparse volterra series. *Journal of Aircraft*, 49(6).

[7] Zhang, W., Wang, B., Ye, Z., et al. (2012). Efficient method for limit cycle flutter analysis by nonlinear aerodynamic reduced-order models. *AIAA Journal*, 50(5).

[8] Mannarino, A. and Mantegazza, P. (2014). Nonlinear aeroelastic reduced order modeling by recurrent neutral networks. *Journal of Fluids and Structures*, 48, 103–121.

[9] Ueda, T. and Dowell, E. (1984). Flutter analysis using nonlinear aerodynamic forces. *Journal of Aircraft*, 21(2).

[10] He, S., Yang, Z., and Gu, Y. (2014). Transonic limit cycle oscillation analysis using aerodynamic describing functions and superposition principle. *AIAA Journal*, 52(7).

[11] van der Pol, B. (1927). Forced oscillations in a circuit with nonlinear resistance (receptance with reactive triode). *London, Edinburgh and Dublin Phil. Mag.*, 3, 65–80.

[12] Schewe, G., Knipfer, A., Mai, H., et al. (2002). Experimental and numerical investigation of nonlinear effects in transonic flutter. Internal Report DLR IB 232 - 2002 J 01, Deutsches Zentrum für Luft- und Raumfahrt e.V. (DLR), Institut für Aeroelastik, Göttingen, Germany.

[13] Schewe, G., Mai, H., and Dietz, G. (2003). Nonlinear effects in transonic flutter with emphasis on manifestations of limit cycle oscillations. *Journal of Fluids and Structures*, 18, 3–22.

[14] Dietz, G., Schewe, G., Kiessling, F., et al. (2003). Limit-cylce-oscillation experiments at a transport aircraft wing model. Amsterdam, The Netherlands: Deutsches Zentrum für Luft- und Raumfahrt, Institut für Aeroelastik. International Forum on Structural Dynamics and Aeroelasticity (IFASD).

[15] Dietz, G., Schewe, G., and Mai, H. (2004). Experiments on heave/pitch limit-cycle oscillations of a supercritical airfoil close to the transonic dip. *Journal of Fluids and Structures*, 19, 1–16.

[16] Dietz, G., Schewe, G., and Mai, H. (2006). Amplification and amplitude limitation of heave/pitch limit-cycle oscillations close to the transonic dip. *Journal of Fluids and Structures*, 22, 505–527.

[17] Weber, S., Jones, K., Ekaterinaris, J., et al. (1999). Transonic flutter computations for a 2d supercritical wing. A99-16647. Reno, NV: Naval Postgraduate School, Monterey, CA. 37th AIAA/ASME/ASCE/AHS/ASC Structures, Structural Dynamics, and Materials Conference and Exhibit.

[18] Castro, B., Jones, K., Ekaterinaris, J., et al. (2001). Analysis of the effect of porous wall interference on transonic airfoil flutter. Anaheim, CA: Naval Postgraduate School, Monterey, CA. 31st AIAA Fluid Dynamics Conference & Exhibit.

[19] Tang, L., Bartels, R., Chen, P., et al. (2003). Numerical investigation of transonic limit cycle oscillations of a two-dimensional supercritical wing. *Journal of Fluids and Structures*, 17, 29–41.

[20] Wang, B. and Zha, G.-C. (2010). Numerical simulation of transonic limit cycle oscillations using high-order low-diffusion schemes. *Journal of Fluids and Structures*, 26, 579–601.

[21] Thomas, J., Dowell, E., and Hall, K. (2002). Modeling viscous transonic limit cycle oscillation behavior using a harmonic balance approach. Denver, CO: Duke University, Durham, NC. 43rd AIAA/ASME/ASCE/AHS/ASC Structures, Structural Dynamics, and Materials Conference and Exhibit.

[22] Thomas, J., Dowell, E., and Hall, K. (2003). Modeling limit cycle oscillations for an nlr 7301 airfoil aeroelastic configuration including correlation with experiment. AIAA 2003-1429. Norfolk, VA: Duke University, Durham, NC. 44th AIAA/ASME/ASCE/AHS/ASC Structures, Structural Dynamics, and Materials Conference and Exhibit.

[23] Weber, S., Jones, K., Ekaterinaris, J., et al. (2001). Transonic flutter computations for the nlr 7301 supercritical airfoil. *Aerosp. Sci. Technology*, 5, 293–304.

[24] Tang, L., Bartels, R., Chen, P., et al. (2001). Simulation of transonic limit cycle oscillations using a cfd time-marching method. AIAA 2001-1290. Seattle, WA. 42nd AIAA/ASME/ASCE/AHS/ASC Structures, Structural Dynamics, and Materials Conference and Exhibit.

[25] Bendiksen, O. (2004). Transonic limit cycle flutter/lco. AIAA 2004-1694. Palm Springs, California: Univerisity of California, Los Angelos. 45th AIAA/ASME/ASCE/AHS/ASC Structures, Structural Dynamics, and Materials Conference.

[26] Saitoh, K. and Kheirandish, H. (2007). Numerical simulation of small amplitude lco for nlr-7301 profile. Stockholm, Sweden. International Forum on Structural Dynamics and Aeroelasticity (IFASD).

[27] Saitoh, K., Voss, R., and Kheirandish, H. Numerical study of nonlinearity of unsteady aerodynamics for nlr7301 profile.

[28] Schwamborn, D., Gerhold, T., and Heinrich, R. (2006). The dlr tau-code: Recent applications in research and industry. The Netherlands. ECCOMAS CFD conference.

[29] Jameson, A., Schmidt, W., and Turkel, E. (1981). Numerical solutions of the Euler equations by finite volume methods using Runge-Kutta time-stepping schemes. AIAA Paper 1981-1259.

[30] Jameson, A. (1991). Time dependent calculations using multigrid, with applications to unsteady flows past airfoils and wings. *AIAA Paper 91-1596*. AIAA 10th Computational Fluid Dynamics Conference.

[31] Zwaaneveld, J. (1979). Nlr 7301 airfoil. In *EXPERIMENTAL DATA BASE FOR COMPUTER PROGRAM ASSESSMENT - Report of the Fluid Dynamics Panel Working Group 04*, AGARD-AR-138. pp. A4–1–A4–22.

[32] van Rooij, A., Nitzsche, J., Bijl, H., et al. (2013). Limit-cycle oscillations of a supercritical airfoil. Bristol, UK. International Forum on Structural Dynamics and Aeroelasticity (IFASD).

[33] van Rooij, A., Nitzsche, J., and Dwight, R. (2015). Harmonic forced motion oscillations for modelling and analysing aeroelastic limit-cycle oscillations of a two-degree-of-freedom airfoil system. In preparation.

[34] Hassig, H. (1971). An approximate true damping solution of the flutter equation by determinant iteration. *Journal of Aircraft*, 8(11).

[35] Lophaven, S., Nielsen, H., and Søndergaard, J. (2002). Daca - a matlab kriging toolbox. Tech. Rep. IMM-TR-2002-12, Informatics and mathematical modelling, Technical University of Denmark.

[36] Sacks, J., Welch, W., Mitchell, T., et al. (1989). Design and analysis of computer experiments. *Statistical Science*, 4(4), 409–435.

6 COPYRIGHT STATEMENT